S. Raghavendran, B. Chitti Babu* and Luigi Piegari

Analysis, Design and Experimental Validation of Modified Simple Soft Switching DC-DC Boost Converter

DOI 10.1515/ijeeps-2015-0013

Abstract: This paper investigates a modified simple soft switching dc-dc converter for low power applications. This simple topology uses an auxiliary switch, an inductor and a capacitor to operate the converter without switching losses. The efficiency of the converter is improved by transferring the energy that would be dissipated during the switching to the load. The main switch turns-on with zero current switching (ZCS) and turns-off with zero voltage switching (ZVS), while the auxiliary switch turns-on and turns-off with zero voltage switching (ZVS). The detailed theoretical analysis and the design equations are described. In addition to that, the analysis of proposed converter is demonstrated by both simulation and experimental results for effectiveness of the study.

Keywords: soft switching, dc-dc boost converter, zero voltage switching (ZVS), zero current switching (ZCS), switching loss, hard switching

1 Introduction

DC-DC power converters are widely used in many applications and their diffusion has been increased by the diffusion of distributed generation systems. For this reason, high efficiency and low size are becoming targets more and more important for DC-DC power converters. In order to minimize the size of conventional DC-DC converter, the converter switch must be operating at high switching frequency which usually causes higher switching losses [1]. Hence the hard switching dc-dc converter limits the energy transfer efficiency. In order to overcome these drawbacks, the soft switching techniques are employed and different methods of soft switching were proposed in recent literature [1–5]. Sang-Hoon Park et al. proposed a soft switching boost converter using a simple auxiliary resonant circuit for a PV system. The auxiliary resonant circuit helps the main switch operate with ZCS and ZVS. However the circuit has two auxiliary diodes that will results in increased conduction losses. In Ref. [2] a soft switching boost converter using an auxiliary resonant circuit was proposed. However the converter structure and the control are complex. Soft switching using coupled inductors were achieved in Refs [3–5]. An auxiliary switch along with a coupled inductor and a diode is utilized to obtain soft switching in Ref. [3]. The improved topology was introduced in Ref. [4]. In both the topologies, reduced current and voltage stress of the switch were achieved only for large values of resonant impedance and turns ratio of the coupled inductor. The presence of bulky inductor results in poor dynamic response. Moreover the over-voltage due to the energy stored in the leakage inductor deteriorates the efficiency of the converter [6]. This requires additional intermediate energy recycling stage that complicates the circuit operation. A passive non-dissipative turn-on turn-off snubber is used in Ref. [7], to improve the performance of MPP tracker in PV systems. The efficiency of the power converter is increased to 4% using the snubber circuit. However the snubber circuit is complex and contains too many auxiliary diodes. A boost converter with fly back snubber was proposed in Ref. [8]. A complex fly back unit was added to the conventional converter to suppress the voltage and current stress. But the increase in the efficiency is just 1%. The isolated DC-DC converter topologies have been proposed in Refs [9–11]. Snubber formed with a capacitor and two switches is utilized to achieve soft switching in Ref. [9]. A step-up DC–DC converter employing an active-clamp circuit for soft switching of the power semiconductor switches is proposed in Ref. [10]. A novel topology is proposed for the photovoltaic DC/DC converter to achieve high efficiency for wide load ranges. The circuit topologies are complex and the efficiency claimed is normally less than the non-isolated converters. The use of a switched capacitor dc–dc converter for

***Corresponding author: B. Chitti Babu,** Centrum ENET, VSB-Technical University of Ostrava, 708 33–Ostrava-Poruba, Czech Republic, E-mail: bcbabunitrkl@gmail.com
S. Raghavendran, Department of Electrical Engineering, National Institute of Technology, Tiruchirappalli 620015, India, E-mail: raghavagi@gmail.com
Luigi Piegari, Department of Electronics, Information and Bioengineering, Politecnico di Milano, Italy, E-mail: luigi.piegari@polimi.it
http://orcid.org/0000-0003-3776-7486

tracking the maximum power point of a photovoltaic array is proposed in Ref. [12]. The switched capacitor converters though having the advantage of absence of inductors and transformers, high voltage stress across the switch is major drawback in these converters.

To improve the performance and reduce the complexity in DC-DC converter, this paper presents a novel soft-switching dc-dc boost converter using a resonant circuit with an active switch. The proposed dc-dc converter achieves high energy transfer efficiency with low voltage stress by employing ZCS during turn-on and ZVS during turn-off for the main switch and ZVS for the auxiliary switch. The operating principles of each mode are analyzed and a detailed design procedure of the proposed soft switching boost converter is presented. In addition to that, the analysis of proposed converter is demonstrated by both simulation and experimental results for effectiveness of the study.

2 Analysis of proposed soft switching converter

The circuit diagram of proposed soft switching boost converter employing an active switch and the resonant circuit is shown in Figure 1.

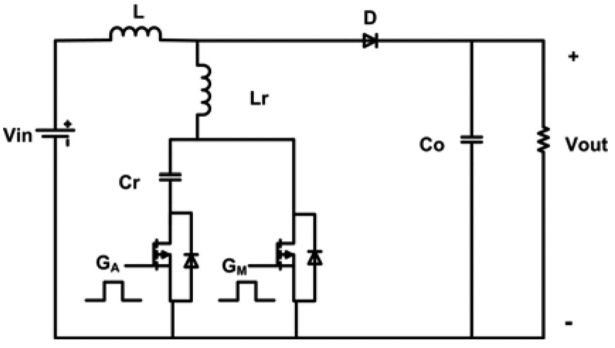

Figure 1: Circuit diagram of proposed dc-dc soft switching boost converter.

The following assumptions are made to simplify the steady-state analysis of the circuit.

1. All switching devices and passive elements are ideal.
2. The parasitic components of all switching devices and elements are neglected.

The operating principle of proposed soft switching converter is divided into 7 modes as shown in Figure 2. The key waveforms for the different modes of operation are shown in Figure 3.

2.1 Mode 1($t_o \le t \le t_1$)

In the first operating mode the main switch and the auxiliary switch are in off state. The input is connected directly to the output through the main inductor and output diode.

$$i_L(t) = i_D(t) = i_c(t) + Io \tag{1}$$

$$I_{Lr}(t) = 0 \tag{2}$$

$$V_{cr}(t) = 0 \tag{3}$$

2.2 Mode 2($t_1 \le t \le t_2$)

This mode starts with turning on of the main switch at time t_1. The main switch turns on under zero current switching (ZCS) because of the resonant inductor. The output diode current reaches zero at time t_2 when the resonant inductor current reaches the main inductor current.

$$i_L(t) = i_D(t) + i_{Lr}(t) \tag{4}$$

$$i_{Lr}(t) = \frac{Vo}{L_r}t \tag{5}$$

$$i_L(t_2) = i_{Lr}(t_2) \tag{6}$$

$$i_D(t_2) = 0 \tag{7}$$

2.3 Mode 3($t_2 \le t \le t_3$)

In this mode the input side of the converter is isolated from the output side of the converter. The main inductor is charged from the input source. The inductor current rises from the minimum value towards the maximum value. The resonant inductor current is same as that of the main inductor current.

$$i_L(t_2) = I_{\min} \tag{8}$$

$$i_L(t) = I_{min} + \frac{Vs}{L + L_r}t \tag{9}$$

2.4 Mode 4($t_3 \le t \le t_4$)

The auxiliary switch is turned on under zero voltage switching (ZVS) in this mode. The voltage across the auxiliary switch is clamped to zero by the already

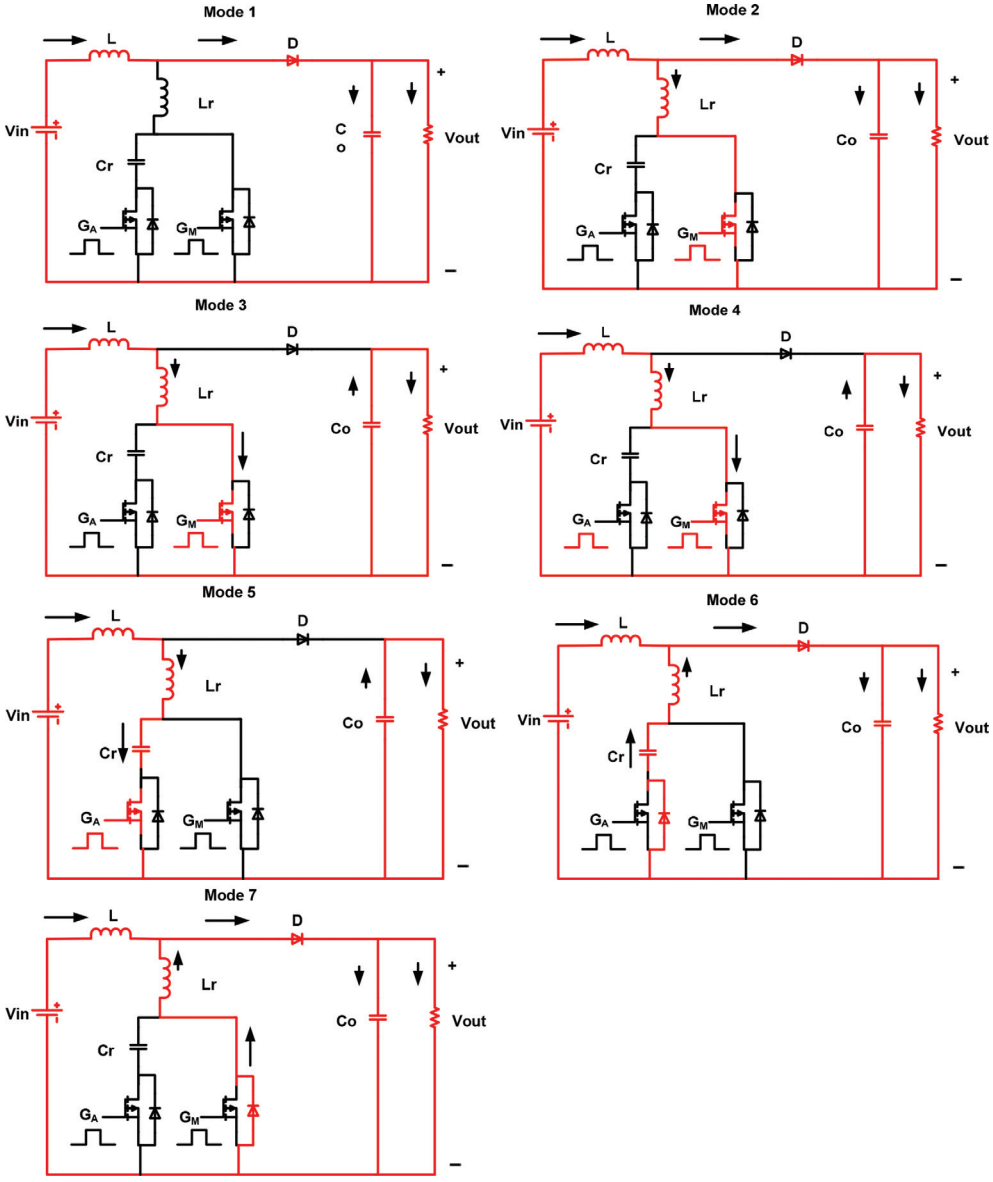

Figure 2: Modes of operation of proposed soft switching boost converter.

conducting main switch. There will be no current flow through the auxiliary switch – resonant capacitor branch.

2.5 Mode 5($t_4 \le t \le t_5$)

To begin with this mode, the main switch is turned off under zero voltage condition at t_4. The resonance between the resonant inductor L_r and the capacitor C_r starts. The voltage across the resonant capacitor begins to rise, meanwhile the current through the resonant inductor begins to fall and it reaches zero, when the capacitor is charged to maximum value. This mode acts as charging mode of the capacitor.

$$w_o = \frac{1}{\sqrt{L_r C_r}} \tag{10}$$

$$z_o = \sqrt{\frac{L_r}{Cr}} \tag{11}$$

$$iL_r(t_4) = I_{Lmax} = I_{Lrmax} \tag{12}$$

$$iL_r(t) = I_{Lrmax} cosw_o t \tag{13}$$

$$V_{cr}(t) = V_{crmax} sinw_o t \tag{14}$$

$$V_{crmax} = \frac{I_{Lrmax}}{w_o.C} \tag{15}$$

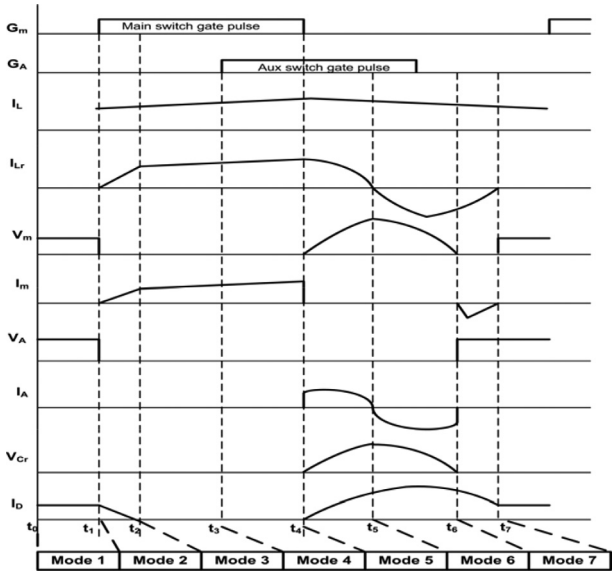

Figure 3: Key waveforms of proposed soft switching boost converter.

2.6 Mode 6($t_5 \le t \le t_6$)

This mode is discharging mode of the capacitor. The capacitor discharges its stored energy to the output through the resonant inductor Lr, the output diode D and the anti-parallel diode of the auxiliary switch to the load. The direction of the current through the resonant inductor is reversed. Now the current through the resonant inductor is the discharging current of the resonant capacitor. The auxiliary switch is turned off under zero voltage condition (ZVS). This mode lasts when the resonant capacitor is fully discharged.

$$i_{cr}(t) = -(V_0 - V_{crmax})cosw_o t \tag{16}$$

$$i_{Lr}(t) = i_{cr}(t) \tag{17}$$

$$i_L(t) + i_{Lr}(t) = i_D(t) \tag{18}$$

$$V_{cr}(t_6) = 0 \tag{19}$$

2.7 Mode 7($t_6 \le t \le t_7$)

The energy stored in the resonant inductor is transferred to the load through the main diode and the anti-parallel diode of the main switch. This mode ends when the resonant inductor discharges completely.

$$i_{Lr}(t) = i_{Lr}(t_6) - \frac{Vo}{L_r}t \tag{20}$$

$$i_{Lr}(t_7) = 0 \tag{21}$$

3 Design procedure for resonant inductor and capacitor

The current through the resonant inductor rises from zero to main inductor current value between time t_2–t_3. The time interval t_2–t_3 is selected as 10% of the D_{min}. In this time interval the change in the current through the resonant inductor is from zero to I_{min}.

$$\Delta i_{Lr} \cong I_{\min} \tag{22}$$

$$\Delta t = t_3 - t_2 = 0.1\,D_{min} \tag{23}$$

$$L_r = \frac{Vo}{\Delta i_{Lr}}\Delta t \tag{24}$$

The value of resonant inductor can be chosen from eq. (24).

The time t_4–t_6, i.e., the time for half resonant cycle is selected as 10% of the total time period.

$$\Delta t = t_6 - t_4 = \frac{0.10}{fsw} = \frac{T_r}{2} \tag{25}$$

$$f_r = \frac{1}{T_r} = \frac{1}{2\pi\sqrt{L_r\,C_r}} \tag{26}$$

$$C_r \langle \frac{1}{4\pi^2 L_r f_r} \tag{27}$$

From eq. (27) C_r can be calculated.

The auxiliary switch is turned off anywhere between t_5 and t_6. So, the phase shift between the gate pulses of main switch and auxiliary switch can be chosen to be greater than $T_r/4$ but less than $T_r/2$.

4 Simulation results

The design of proposed soft switching boost converter is validated through computer simulation using PSIM® software. The converter is designed for of 3W power transfer, with the input voltage of 6 V DC. The switching frequency is 30 kHz. The results obtained with the simulation are shown in the following figures.

The gate pulse, voltage and current waveforms of the main switch are shown in Figure 4 and ZCS during turn on and ZVS during turn off can be observed. Figure 5 shows the voltage and current waveforms of auxiliary switch and ZVS during both turn on and turn off is achieved. The input inductor current waveform is shown in Figure 6. The output voltage waveform of the proposed converter

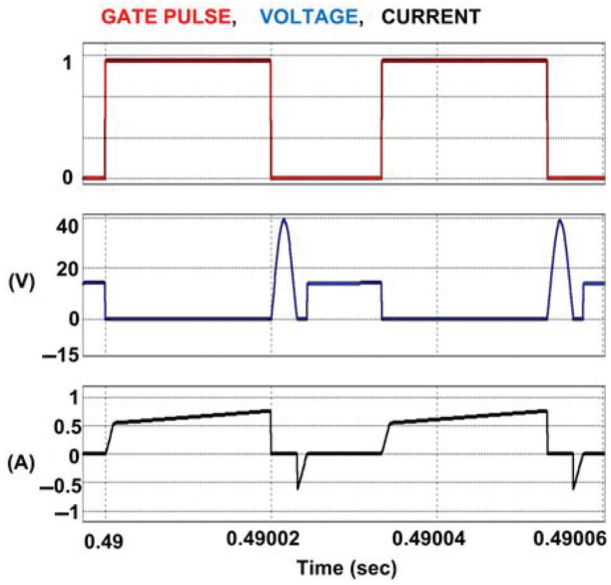

Figure 4: Voltage and current waveform of Main switch.

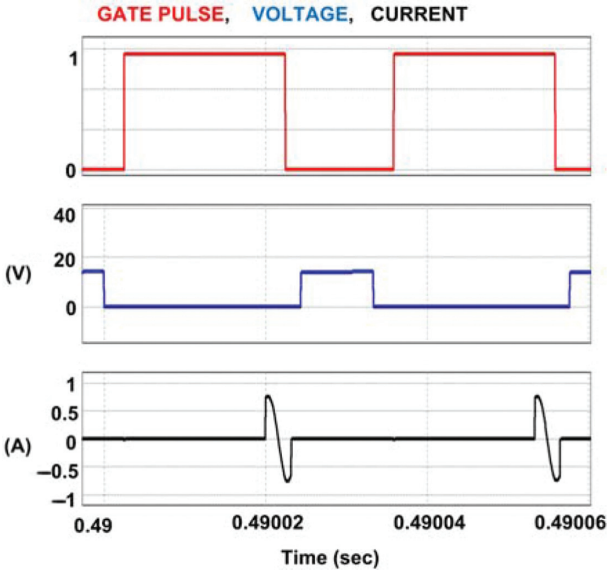

Figure 5: Voltage and current waveform of Auxiliary switch.

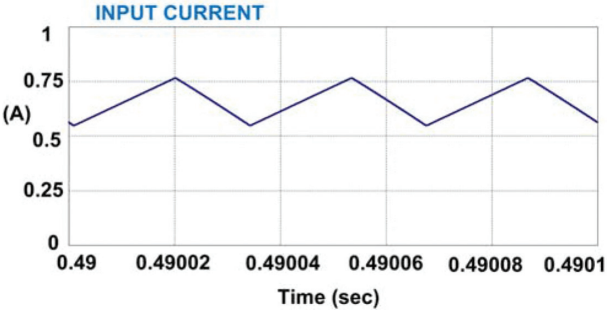

Figure 6: Simulated waveforms of main inductor current.

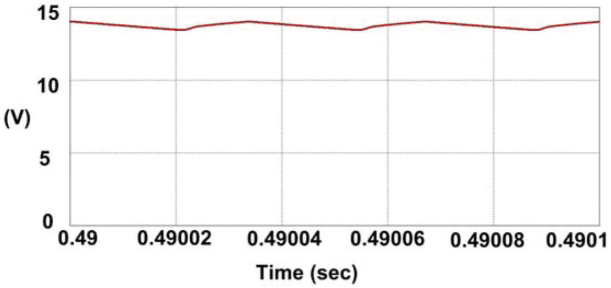

Figure 7: Output voltage waveform of proposed soft switching converter.

is shown in Figure 7.From the waveform the voltage across the load is less than 15V for the duty ratio of 0.6.

5 Experimental results

The prototype of the proposed soft switching converter is shown in Figure 8. The component used for fabricating the proposed converter is listed in Table 1. Switching pulse is generated from the 8,051 micro controller. The rheostat load of 47 Ω is used as 100% load. The output voltage obtained for the input voltage of 6 V and duty cycle of 0.4 is 10 V which is shown in Figure 9. Figure 10 shows the gate pulse, voltage and current waveforms of the main switch. It clearly shows the soft switching achieved during turn-on and turn-off. The peak value of the main switch voltage rises to 3.5 times of the output voltage, which is peak value of resonant capacitor. The body diode of the main switch conducts for a short duration after the capacitor is fully discharged. Then the voltage across the switch is clamped to output voltage. So, the voltage rating of the main switch should be chosen to withstand the peak voltage. The ZVS operation of the auxiliary switch is also obtained in the prototype

Figure 8: Prototype of proposed converter.

Table 1: Component list for prototype model.

Component	Part number
Main switch & Auxiliary switch	IRF 640
Diode	Body diode of IRF 640
Main inductor	500 μH
Resonant inductor	25 μH
Output capacitor	10 μF
Resonant capacitor	22 nF

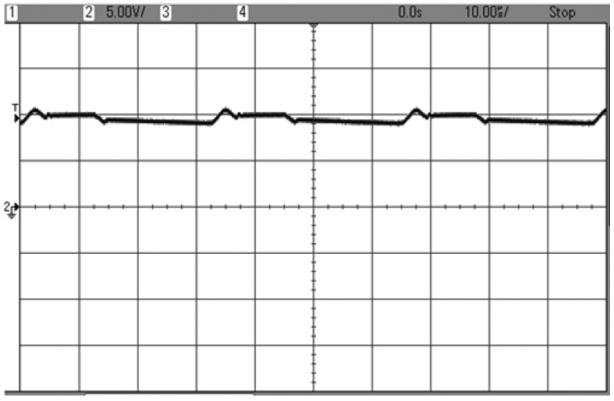

Figure 9: Output voltage.

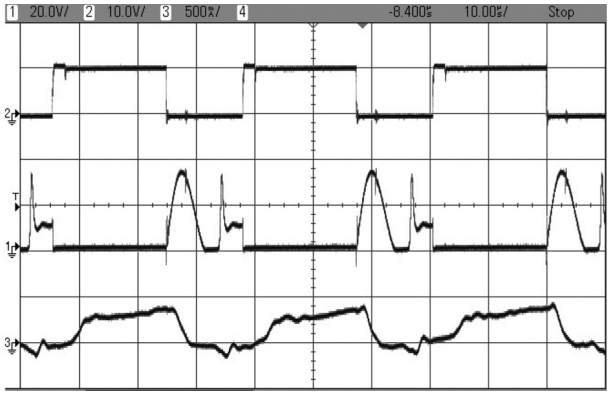

Figure 10: Gate pulse, voltage and current of main switch.

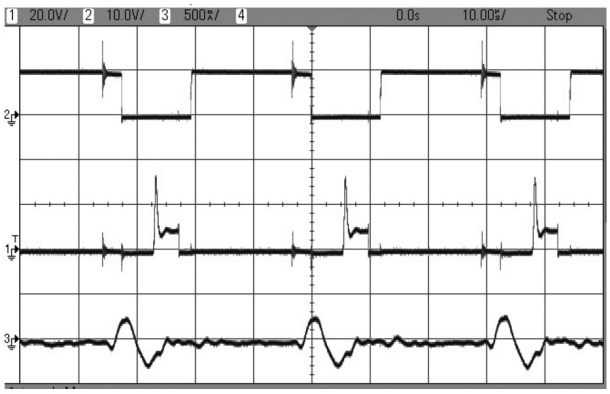

Figure 11: Gate pulse, voltage and current of auxiliary switch.

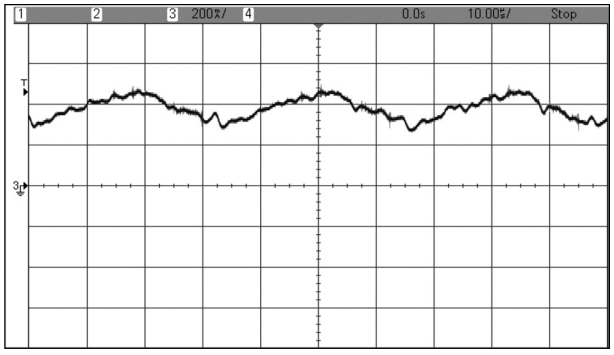

Figure 12: Input current.

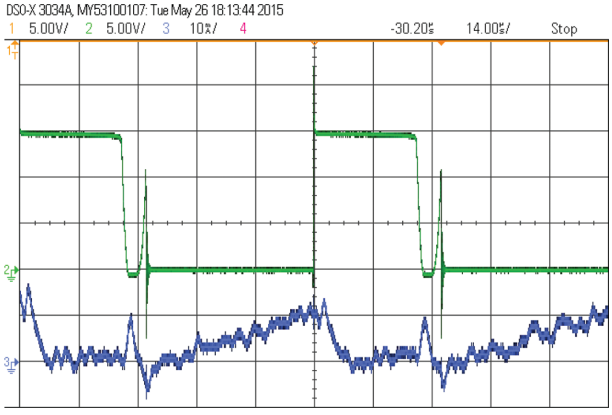

Figure 13: Voltage and current of switch in hard switching converter.

model which is shown in Figure 11. The auxiliary switch voltage is clamped to output voltage. The parasitic in the mosfet results in ringing in the voltage waveform. The current waveforms of the main and auxiliary switch are slightly phase shifted from the respective voltage forms. The delay is caused by the current probe. The input current waveform is shown in Figure 12. The average current is 370 mA. Even though there is reduction in the output voltage for the corresponding duty cycle, there is a reduction in the current drawn from the source which improves the efficiency of the converter. The voltage and current waveforms of hard switching DC-DC boost converter is shown in Figure 13. During the turn-on and turn-off instants of the switch, presence of high voltage and current simultaneously in the switch can be

observed. This leads to very high instantaneous power loss in the switch. The voltage spikes can be observed during turn-on instant of the switch due to the reverse recovery current of the diode. The power loss during switching and high voltage spikes during switching is eliminated in the proposed soft switching converter [13]. The smooth transition of voltage across the switch and current through the switch is achieved in the proposed soft switching converter.

The efficiency curve of the proposed converter is plotted for various load condition with input voltage and duty cycle fixed. The efficiency obtained for load conditions is shown in Figure 14. The proposed converter has better efficiency profile than the conventional boost converter.

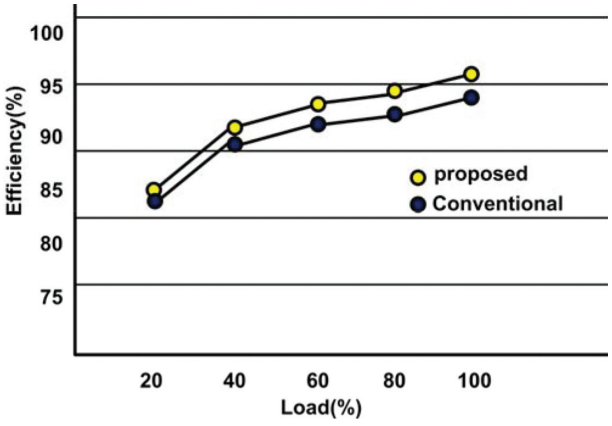

Figure 14: Efficiency comparison.

6 Conclusions

In this paper, a simple soft switching boost converter using an auxiliary switch, an inductor and a capacitor is proposed. The operation modes are divided based on the voltage and current waveforms and the equivalent circuit of each mode of operation is illustrated. The analysis of the proposed soft switching converter in each mode of operation is done through the simulation and experiment. The proposed converter uses less number of components to achieve soft switching. It is verified that the switching of main switch and auxiliary switch is smooth for better efficiency of the converter. This soft switching dc-dc converter can be used in low power applications where there is a necessity of maintaining constant DC-bus voltage. Using this, it will not only result in better symbiotic working conditions and a new area of exploration but the use of proposed soft switching dc-dc boost converter in extraction of the DC power will enhance the efficiency of the proposed system, thus makes the overall system simple and cost effective.

References

1. Park S-H, Cha G-R, Jung Y-C, Won C-Y. Design and application for PV generation system using a soft-switching boost converter with SARC. IEEE Trans Industrial Electron 2010;57: 515–22.
2. Song I-B, Jung D-Y, Ji Y-H, Choi S-C, Jung Y-C, Won C-Y, A Soft Switching Boost Converter using an Auxiliary Resonant Circuit for a PV System, 8th International Conference on Power Electronics – ECCE Asia 2011, 2011:2838–43.
3. Adib E, Farzanehfard H. Family of soft-switching PWM converters with current sharing in switches. IEEE Trans Power Electron 2009;24:979–85.
4. Amini MR, Farzanehfard H. Novel family of PWM soft-single-switched DC–DC converters with coupled inductors. IEEE Trans Ind Electron 2009;56:2108–14.
5. Do H-L. Zero-voltage-switching boost converter using a coupled inductor. J Power Electron 2011;11:16–20.
6. Pierre Petit, Abdallah Zgaoui, Jean-Paul Sawicki, Michel Aillerie and Jean-Pierre Charles. New architecture for high efficiency DC-DC converter dedicated to photovoltaic conversion. Energy Procedia 2011;6:688–94.
7. Santos JL, Antunes F, Chehab A, Cruz C. A maximum power point tracker for PV systems using a high performance boost converter. Solar Energy 2006;80:772–8.
8. Wu T-F, Chang Y-D, Chang C-H, Yang J-G. Soft-switching boost converter with a flyback snubber for high power applications. IEEE Trans Power Electron 2012;27:1108–19.
9. Huai Wang, Qian Sun, Henry Shu Hung Chung, Saad Tapuchi, and Adrian Ioinovici. A ZCS current-fed full-bridge PWM converter with self-adaptable soft-switching snubber energy. IEEE Trans Power Electron 2009;24:1977–91.
10. Kwon J-M, Kwon B-H, Nam K-H. High-efficiency module-integrated photovoltaic power conditioning system. IET Power Electron 2009;2:410–20.
11. Lee J-P, Min B-D, Kim T-J, Yoo D-W, Yoo J-Y. Design and control of novel topology for photovoltaic DC/DC converter with high efficiency under wide load ranges. J Power Electron 2009;9:300–7.
12. Peter PK, Agarwal V. On the input resistance of a reconfigurable switched capacitor DC–DC converter-based maximum power point tracker of a photovoltaic source. IEEE Trans Power Electron 2012;27:4880–93.
13. Raghavendran S, Chitti Babu B. Performance improvement of soft switching DC-DC boost converter for photovoltaic (PV) applications. J Low Power Electron 2014;10: 58–64.